NINTH INTERNATIONAL SYMPOSIUM ON

APPLICATIONS OF LASER TECHNIQUES TO FLUID MECHANICS

VOLUME I

July 13th - 16th 1998
Lisbon, Portugal

ENERGY LOSSES ON A 90° TEE JUNCTION

R. Maia[1], F. T. Pinho[2], M. F. Proença[1] and A. Schulte[3]

[1] Department of Civil Engineering, Faculdade de Engenharia, Universidade do Porto, Portugal
[2] Department of Mechanical Engineering, Faculdade de Engenharia, Universidade do Porto, Portugal
[3] INEGI- Instituto de Engenharia Mecânica e Gestão Industrial, Portugal

ABSTRACT

The flow in a 90° tee junction with sharp edges is investigated in detail by means of LDA techniques for an inlet Reynolds number of 32 000 and a flow rate ratio of 50%. A strong recirculation zone was found attached to the upstream wall of the branch pipe and the shear layer that formed in the middle of the pipe was responsible for the highest levels of turbulence. No separation was detected in the straight outlet pipe. Mean flow measurements in a similar tee with a rounded edge at the bifurcation showed a shorter, thinner and weaker recirculation bubble, which suggests that a lower loss coefficient will be measured.

1. INTRODUCTION

The flow in pipe network systems is of great engineering importance due to its widespread industrial applications as in fluid transport and heating and its proper design requires the knowledge of pressure losses in pipes, as well as fittings and accessories. As far as pressure losses in straight pipes are concerned there is an established knowledge in the literature, except for cases involving new fluids of non-Newtonian characteristics (Gyr and Bewersdorff, 1995). For pressure losses in fittings and accessories there is also a wide range of information available in the literature (Idel'cik, 1986 and Miller, 1986), but the accuracy of the results is not so high. In fact, (1) most of the data were obtained in the early half of the century, (2) there is lack of data for some flow configurations and (3) the energy loss coefficients not always follow a consistent definition.

One of the more complex accessories is the bifurcation and the present work is aimed at investigating the flow in a 90° tee junction. The first systematic experimental work in this geometry was carried out in Munich by Vogel (1928). Gardel (1957) extended the analysis to include the effects of area ratio and curvature of the junction. Also, Boldy's (1970) work and Ito and Imai's (1973) systematic experimental study on the effect of rounding the junction corner for a 90° tee should be emphasised. Their work is on the basis of the energy loss coefficient values for a tee proposed by the British Hydromechanics Research Association (Miller, 1986). Most of these works are quoted throughout this paper. Although not explicitly referenced, most recent research on bifurcating flows aiming at two-phase fluids as well as biomechanical systems, such as the human and animal circulatory system, must also be referred.

The project of more energy efficient systems requires the optimisation in the design of fluid transport networks and this is the ultimate goal of the present work. In particular, this paper is part of a research project aimed at investigating the effect of geometrical changes on the energetic performance of 90° flow bifurcations operating with both Newtonian and non-Newtonian fluids. The project follows previous work by Maia (1992), who concluded that the traditional pressure field characterisation is no longer enough to improve the design of the pipe accessories, but requires a deeper knowledge of the relationship between flow geometry, pressure field and flow kinematics. In the present contribution, the flow is fully characterised for one flow configuration in a sharp edged tee but some recent results of the mean flow in one rounded-edge tee for the same flow conditions are also included.

The paper is organised as follows: in the next section the rig and instrumentation are described and the experimental uncertainties quoted. Then, the results of pressure measurements for the sharp-edge tee are presented and are followed by a detailed mean and turbulent flow characterisation, where a brief comparison with new data for a rounded-edge tee is

included. A summary of the main findings and of future work closes the paper.

2. TEST RIG AND INSTRUMENTATION

The experiments were carried out in the closed circuit rig schematically shown in Fig. 1. The 90° tee junction was inserted at the intersection of three 2.6 to 2.8 m long pipes of 30 mm internal diameter. The water flow was driven by a volumetric Mohno pump supplied by a tank with constant head regulation by means of an overflow tube. A variable speed controller operated the pump and three inflow/outflow valves enabled to study all possible flow configurations up to a Reynolds number of 32 000 in the main pipe. In this paper, only the configuration of inflow in the straight pipe and 50% out flowrates in the straight and branch pipes will be investigated.

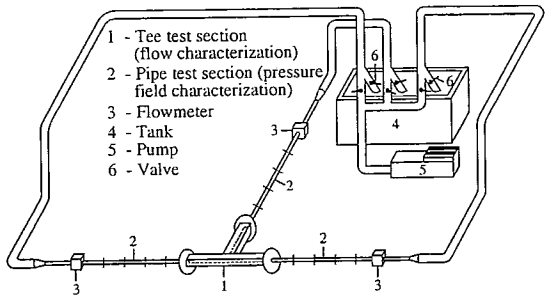

Figure 1- Schematic representation of the experimental set-up.

The flowrate was monitored by three magnetic flowmeters, one in each pipe. The temperature of the water was monitored by means of a PTC100 sensor located in the tank and kept between 15 and 20°C.

The leading pipes and the tee were manufactured of transparent acrylic to allow the use of optical diagnostic tools. The last 30 to 35 diameters approaching the bifurcation and the tee were machined from a block with an external square outer cross section of 50 x 50 mm^2 in order to reduce optical diffraction. The reference tee geometry has sharp-edges whilst the second tee has a rounded edge with a ratio of radius of curvature to pipe diameter of 0.1.

Pressure measurements were performed on seven measuring planes in each of the three 2 m long pipes adjacent to the bifurcation flow field characterisation area (Fig. 1); each pressure section had four pressure taps uniformly distributed around the pipe and was connected to a valve switch board leading to a differential pressure transducer which was interfaced with a computer via an AD converter. The overall uncertainty of the flowrate measurements varied between 2.5% and 0.6% for low and high flowrates, respectively.

Table 1 - Laser-Doppler characteristics

Laser wavelength	820 nm
Laser power	100 mW
Measured half angle of beams in air	3.81°
Size of measuring volume in water (e^{-2} int.)	
minor axis	37 μm
major axis	550 μm
Fringe spacing in air	6.31 μm
Frequency shift	1.0 MHz

The velocity measurements relied on a miniaturised fiber optics laser-Doppler velocimeter from INVENT, model DFLDA, similar to that described by Stieglmeier and Tropea (1992), with a 120 mm front lens mounted onto the 30 mm diameter probe. Scattered light was collected by a photodiode in the forward- and back-scatter modes, depending on optical access; the main characteristics of the anemometer are listed in Table 1. The signal was processed by a TSI 1990C counter interfaced with a computer via a DOSTEK 1400A card, which provided the statistical quantities. The maximum uncertainties in the longitudinal mean and rms velocities at a 95% confidence level are, respectively, of 1.1% and 2.7% in low turbulence regions and of 1.6% and 5.5% in high turbulence regions. The uncertainty of the transverse mean and rms velocity components is 1.3% and 6.0% in low and high turbulence regions, respectively. The curvature of the pipe walls was duly accounted for in both the positioning of the control volume and in the value of the conversion factor.

The velocimeter was mounted on a milling table with movement in the three coordinates and the positional uncertainty was ± 100 μm in all three directions.

3. RESULTS AND DISCUSSION

3.1 Pressure Field Characterisation

According to Fig. 2, which also presents the system of coordinates to be used hereafter, the energy balances applied to each of the two possible flow paths on the investigated horizontal non-symmetrical flow configuration yields

$$\frac{p_3}{\rho g}+\frac{U_3^2}{2g}-\frac{p_1}{\rho g}-\frac{U_1^2}{2g}=\lambda_3\frac{l_3}{d_3}\frac{U_3^2}{2g}+\lambda_1\frac{l_1}{d_1}\frac{U_1^2}{2g}+\frac{\Delta p_{3\text{-}1}}{\rho g} \quad (1)$$

and

$$\frac{p_3}{\rho g}+\frac{U_3^2}{2g}-\frac{p_2}{\rho g}-\frac{U_2^2}{2g}=\lambda_3\frac{l_3}{d_3}\frac{U_3^2}{2g}+\lambda_2\frac{l_2}{d_2}\frac{U_2^2}{2g}+\frac{\Delta p_{3-2}}{\rho g} \quad (2)$$

where l_i, p_i and U_i are the distance from fully developed flow cross sections on pipe i to the point of intersection of the three pipes, the static pressure and the bulk mean velocities on those cross sections, respectively; λ_i and d_i represent Darcy's friction factor and the diameter of pipe i and Δp_{3-1} and Δp_{3-2} are the apparent local pressure losses between the main pipe (3) and the branch (1) and the straight (2) pipes, respectively. Pressure measurements on the fully developed flow regions in each pipe evaluated the friction factor λ_i and the apparent pressure variation due to the tee was determined by application of equations (1) and (2) to the whole set of pressure measurements.

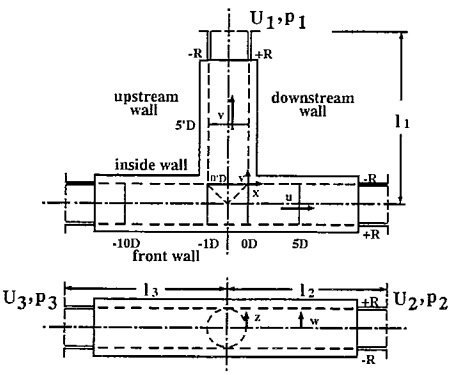

Figure 2- Flow configuration and coordinate system in the tee-junction.

Measurements of the pressure field along the pipes for the sharp-edge tee and the flow configuration in Fig. 2 were carried out for inlet pipe Reynolds numbers in the range $5\,000 \le Re \le 32\,000$ and for the flow rate ratio (Q_1/Q_3) varying from 0 to 1.0. Expressing the local energy losses in terms of the bulk velocity in the main pipe (referred <u> in later sections) the evaluation of the apparent pressure variations Δp_{3-1} and Δp_{3-2} defined above enable the quantification of corresponding local loss coefficients K_{31} and K_{32} which are defined by

$$K_{31} \equiv \frac{\Delta p_{3-1}}{\frac{1}{2}\rho U_3^2} \quad \text{and} \quad K_{32} \equiv \frac{\Delta p_{3-2}}{\frac{1}{2}\rho U_3^2} \quad (3)$$

The variation of loss coefficient K_{31} with the flowrate ratio Q_1/Q_3 for different constant inlet Reynolds number is shown in Fig. 3. The figure includes also information from the literature. Similar presentation of K_{32} would show a better agreement of the same correspondent literature data. To assess the effect of the inlet Reynolds number, the loss coefficient K_{32} is plotted in Figs. 4 for a constant flow rate ratio.

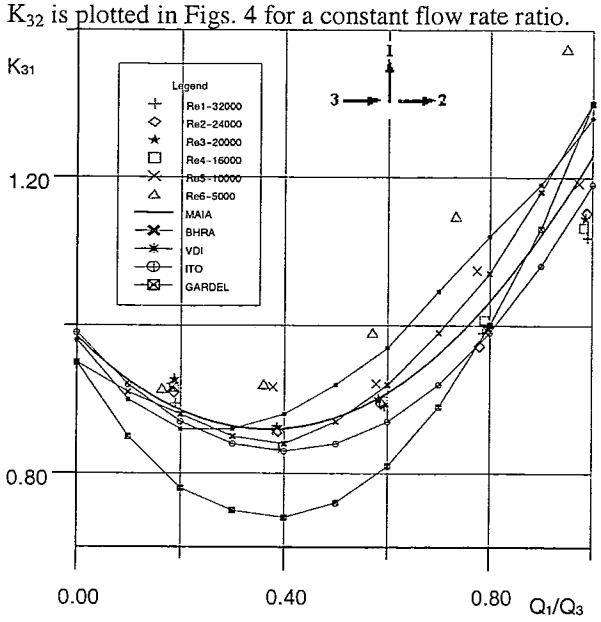

Figure 3- Variation of the local loss coefficient K_{31} in a sharp edge 90° bifurcation as a function of the flow rate ratio for different resultant inlet Reynolds number.

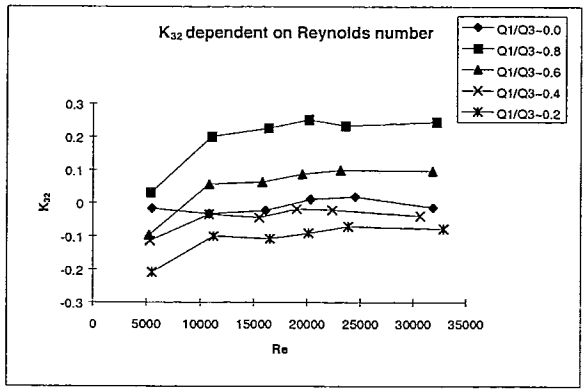

Figure 4- Variation of the local loss coefficient K_{32} (straight flow) in a sharp edge 90° bifurcation with the inlet Reynolds number for a flow rate ratio.

Due to space limitations, both Figs. 3 and 4 refer to different but only one of the two referred loss coefficients. Comparative analysis of all those plots show that the measurements agree well with the literature data at high Reynolds numbers and that the local loss coefficients generically increase (K_{31}) or decrease (K_{32}) as the Reynolds number decreases

towards the transitional regime. The literature data pertains to the high Reynolds number turbulent flow regime, where the local loss coefficient becomes independent of the Reynolds number and this could explain some of the observed discrepancies.

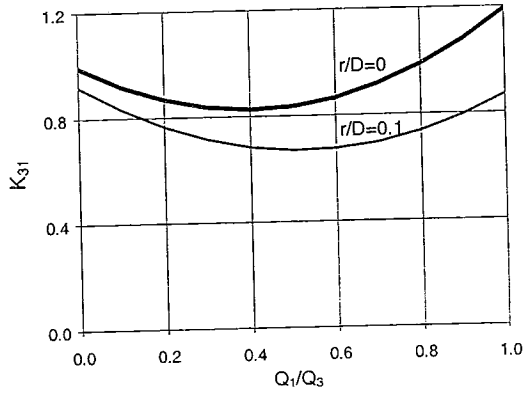

Figure 5- Round-edge effect on local loss coefficient K_{31} (straight flow), according to Ito and Imai (1973).

The pressure field characterisation for the rounded corner geometry (r/D=0.1) has not yet been carried out for this project. Anyway, the correspondent studies presented in the literature permit to foresee that, for the r/D=0.1 round edge, significant effects are expected only in the loss coefficient for the main to side branch, i.e., K_{31}, as can be assessed in Fig. 5. According to Miller (1986) and Ito and Imai (1973), sharp-edged case straight flow coefficient values (K_{32}) can be applied to this case. (r/D=0.1)

3.2 Mean Velocity Field

Fig. 6 presents a vector plot of the x- and y-directions mean velocity components (u and v, respectively) in the horizontal diametral plane for the sharp edge bifurcation. The flow in the inlet pipe becomes fully developed well ahead of the bifurcation; the radial profiles of the axial velocity component and of the normal Reynolds stresses collapse for stations -10D and -5D and compare well with data from the literature, except that the turbulence is slightly higher but this can be accounted for by the Reynolds number effect. The present measurements are for a Reynolds number of 32 000 whereas the data in the literature pertain to higher Reynolds numbers.

The nomenclature used is that in Fig. 2, u and v designate the velocities in the x- and y- directions and we call the readers' attention to the names of the various walls mentioned here, which facilitate the understanding. Note also that u is the longitudinal velocity in the main inlet and outlet pipes whereas v is the transverse velocity. The role of these two velocity components is reversed for the branch pipe. All mean and turbulent velocities have been normalised by the inlet bulk velocity and from now on we always refer to these values. In referring to measuring stations a prime designates the branch pipe, and negative stations are in the inlet pipe (see Fig. 2: 0D and 0'D represent the entrance to the outlet and branch pipes, respectively).

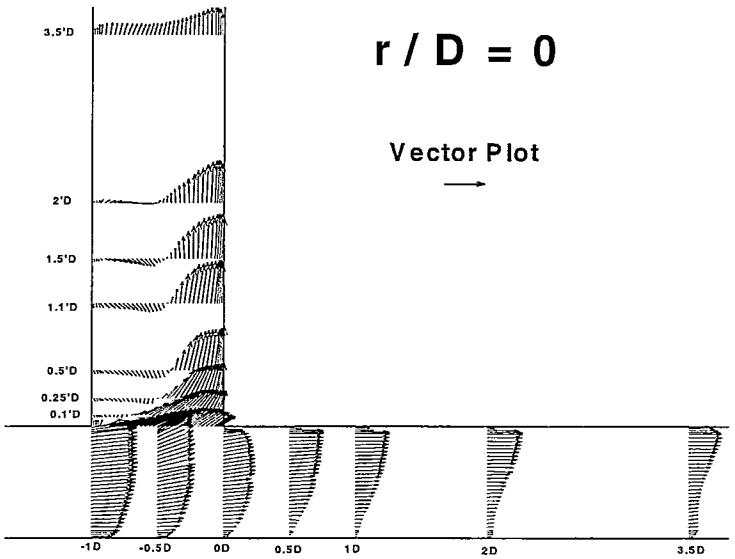

Figure 6- Vector plot of u- and v- mean velocity components in the diametral horizontal plane for the sharp-edge tee bifurcation.

On approaching the beginning of the bifurcation (-1.0D) the flow in the inlet pipe deviates towards the inside wall. In the middle of the bifurcation (-0.5D) the maximum longitudinal velocity has dropped only to about 0.9, indicating that in the first half of the branch pipe the main flow does not deviate significantly towards the side branch. Indeed, the onset of a recirculation zone at the edge of the upstream wall of the branch pipe blocks the passage of fluid which is forced into it only at the downstream half of the cross-section.

The recirculation bubble in the branch pipe is about 2.0D long and, although its maximum width occurs near the entrance, the width remains fairly constant up to about 2.0'D and the maximum longitudinal velocities in the stream occur at 1.5'D. The shape of the bubble at the end of the recirculation is rather strange. At 2.0'D the flow near the upstream wall is already positive but there is still a small negative velocity near the pipe axis. Although this is a turbulent flow, this finding is in agreement with the laminar flow pattern measured by Maia (1992). Close inspection of the vectors inside the recirculating region show also that the flow is moving away from the wall, and continuity requires that an inflow into the wall region must take place. The hint is obvious: we are in the presence of a strong 3D flow with the w velocity component feeding fluid into this region from above and below the diametral plane. This component of the velocity vector has not been measured yet, but these results suggest the need to do it, at least in the branch pipe.

Horizontal transverse velocities in the main and branch pipes are very low everywhere accounting only for flow redevelopment and continuity, the exception being at the entrance of the branch pipe where the flow tends to be aligned at 45° relative to both the x and y axis.

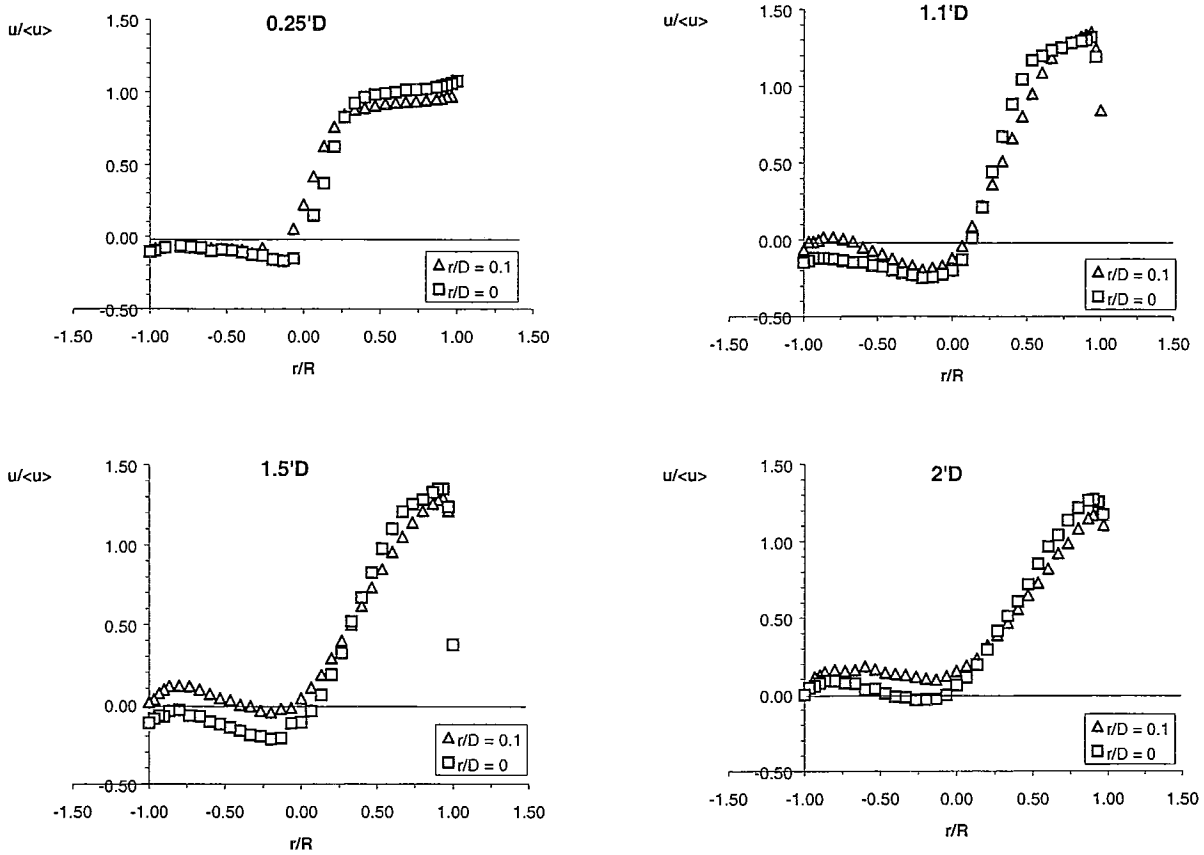

Figure 7- Some horizontal transverse profiles of the longitudinal velocity component in the branch pipe for the sharp and round edged tees.

In the straight outlet pipe the longitudinal velocity profiles are initially skewed towards the inside wall, because of the suction effect of the branch, and then start to redevelop. This is well observed in profiles of the transverse velocity, not shown here, carrying u-momentum from the inside wall region to the vicinity of the outside wall of the main outlet pipe.

It is worth emphasizing that, for this flow rate ratio (50%) there is no flow separation in the main outlet pipe, although we are close to it: an inflection point is clearly identified in the vector profile at 1.0D, near the outside wall. The vertical transverse velocity profiles taken at -0.5D show a second negative velocity region located near the bottom and top walls which we think result from the blockage effect that exists in the passage from the main to the side branch at that location. The intersection of both pipes has an elliptical shape and the main flow into the branch occurs in the middle horizontal diametral section, where cross section areas are larger and thus flow resistance is smaller. The complex 3D flow created at the bifurcation probably generates an adverse pressure gradient near the top and bottom walls which force a small separation.

For the round-edge tee the main flow features remain almost unchanged, with the flow going into the straight pipe not being very affected. Anyhow, comparing the longitudinal velocity profiles of the rounded and sharp edged junctions in the branch pipe (fig. 7) shows that the main effect of the curved edge is to reduce the length, width and strength of the separated flow region. A shorter recirculation bubble in a similar flow situation, but with a different edge curvature, has been observed in the limited experiments of Sierra-Espinosa and Bates (1997) and it suggests that lower energy losses will be measured here for the bifurcated flow.

3.3 Turbulent Velocity Field

Contour plots of the normalised rms of the u and v velocities (u' and v') are presented in Figs. 8 and 9 for the sharp-edge tee, respectively. Measurements of these quantities for the round-edge tee are still under way and therefore are not presented here.

Limitations of space do not allow the presentation of some transverse profiles of u' and v', which would allow an improved understanding of some of the effects. Also, the contour plots are drawn in the horizontal diametral plane, and we are not including here figures describing the variation of the turbulent quantities with the z-direction.

The main turbulent flow features are observed in the bifurcation, the side branch and at the beginning of the outlet straight pipe and they are dominated by the various shear/ boundary layers. Near the inlet of the bifurcation the turbulent flow field has characteristics of a fully developed pipe flow. Then, on entering the bifurcation region there is a shift of the longitudinal mean flow towards the inside wall, with the consequent depletion of fluid and deceleration in the outside wall region of the bifurcation. Flow deceleration contributes positively to turbulence

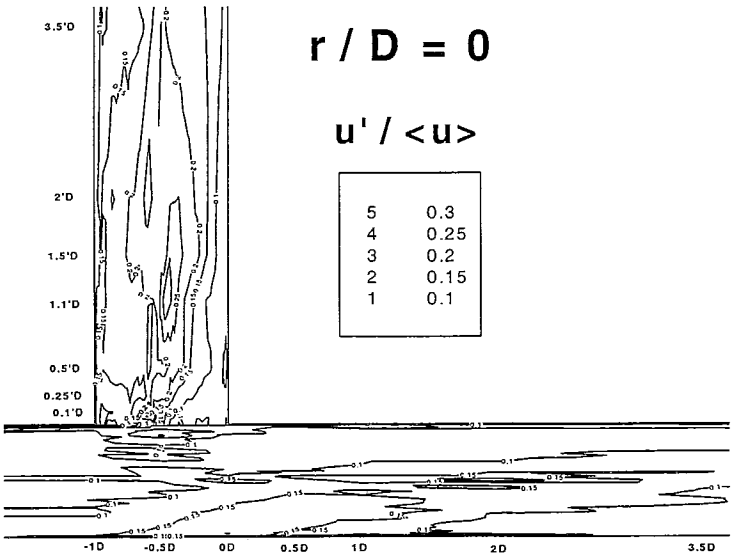

Figure 8 – Contour plots of the normalised turbulence u´/<u> for a sharp-edge tee.

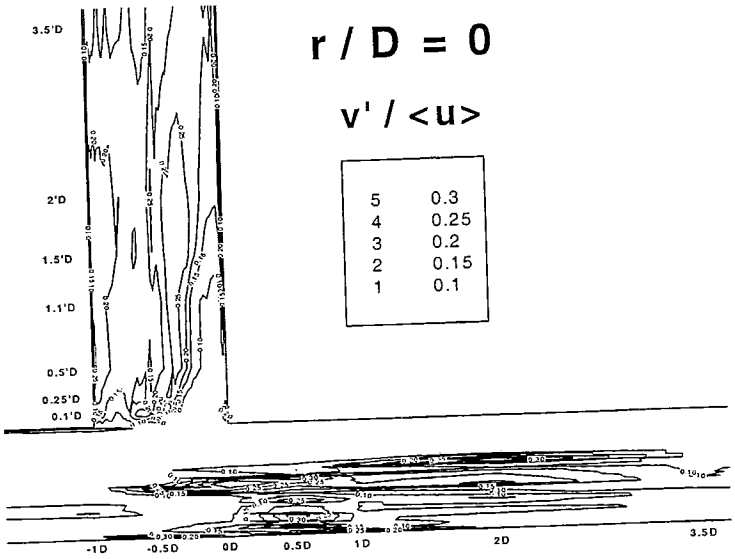

Figure 9 – Contour plots of the normalised turbulence v´/<u> for a sharp-edge tee.

production via a normal rate of strain-normal stress interaction (first term of the right-hand-side of Eq. 4) and hence longitudinal turbulence increases in the outside wall region of the main outlet pipe until about station 1D.

$$\text{Production of } \overline{u'^2} = -\overline{u'^2}\frac{\partial U}{\partial x} - \overline{u'v'}\frac{\partial U}{\partial y} - \overline{u'w'}\frac{\partial U}{\partial z} \qquad (4)$$

Simultaneously, on the inside region the wall has given place to the entrance of the branch pipe with the consequence that suddenly the production of u' by Reynolds shear stress has significantly diminished. The mean flow analysis also shows that in this region the local mean U velocity drops suddenly near the centre of the branch pipe and then it remains fairly constant at a low value because, although flow is exiting to the branch pipe the region is also being fed by fluid from the outside wall region. That sudden local flow deceleration near the entrance to the branch pipe can explain the local maximum in u'. Here there are also gradients of the transverse mean velocity but contours of v' do not show any local maximum.

Going into the outlet pipe there is a reversed behaviour. From about 0.5D to 1.0D, along the outside wall region the shear layer becomes fairly weak because the region has been depleted of fluid and so turbulence production by shear velocity gradient and shear Reynolds stress interaction will be small. Since the longitudinal velocity profile is skewed towards the inside wall, u-momentum will now be transferred from the inside towards the outside wall region, ie., there will be acceleration of fluid in the outside wall region and this represents a sink of turbulence. Both effects, plus the initial peak of u' at inlet and consequent higher turbulent diffusion and turbulence redistribution by pressure strain between 0D and 1.0D will contribute to the decrease of u' at the outside wall region, as the fluid flows downstream. Conversely, at the inside wall the fluid will decelerate and the boundary layer has been re-established, both events contributing to increase turbulence.

The recirculation region in the branch pipe creates a very strong shear layer at its edge, in the centre of the pipe. Here, there is an intense production of longitudinal turbulence (now v') which increases until 1.5D, the station where the mean velocity shear gradient is the steepest and the widest. Note also the peak longitudinal turbulence at the upstream wall of the eddy. This maximum is not locally produced, but represents turbulence generated in the shear layer, which is now being convected into the wall region by the reversed flow. The mean flow analysis has shown that the upstream wall region is being fed by fluid from the locations above and below the horizontal diametral plane and we think that this fluid actually comes from the part of the shear layer in those upper and lower regions of the branch pipe having higher turbulence. This argument is reinforced by the fact that axial

turbulence decays if we move along the upstream wall, towards the entrance of the branch pipe.

Vertical traverses of the longitudinal velocity show also production of turbulence by the wall shear layer at the top and bottom walls in the outlet and side branch pipes, but not so much in the bifurcation region because there, the shear layer is very weak.

For the transverse velocity component (v in the main inlet and outlet pipes and u in the branch pipe) the contours are not very different although for a different reason. With the exception of the entrance to the branch pipe, gradients of the transverse mean velocity are always very small in comparison with gradients of the longitudinal mean velocity. This means that direct production of transverse turbulence will be negligible and so it has to be acquired via a different mechanism, the redistributive role of the pressure strain and possibly turbulent diffusion. So, since the transverse turbulence will acquire its energy from the longitudinal turbulence its variations will follow closely those of the latter. This is exactly what is observed except for the local maxima in the contour plots of v' in the centre of the main outlet pipe which are absent from the contour plot of u'. In this region we experienced difficulties to measure in backscatter due to light reflections and excessive noise, and the data is very scattered. Consequently this particular data should be regarded with suspicion until a new measurement is carried out.

In the bifurcation region, the fluid changes direction especially near the entrance of the branch pipe and both the x- and y- components of the velocity vector become equally important, as well as its corresponding mean velocity gradients. In this region the mean gradients of V become non-negligible and the transverse turbulence starts to increase.

Similar measurements need to be performed for the rounded-edge tee and for both geometries measurements for the z-direction velocity component should be carried out in the region of the recirculation zone in the branch pipe. The two complete sets of data should enable us to relate the pressure and velocity data in order to draw final conclusions regarding the design of more efficient bifurcations.

4. CONCLUSIONS

Detailed measurements of the longitudinal and horizontal transverse mean and turbulent velocities have been carried out in a 90° tee junction for an inlet Reynolds number of 32 000 and a flow rate ratio of 0.5. The flow in the branch pipe is three-dimensional and possesses a recirculation region of complex shape and 2.0D long in the horizontal diametral plane. A strong shear layer exists in the middle of the branch pipe, but most certainly it has a U-shape, and in this region production of turbulence is at its maximum. The flow in the outlet straight pipe did not separate.

In spite of the complex 3-D flow the main features of the turbulent flow field could be explained on the basis of the identification of accelerating/deccelerating flow regions and shear/ boundary layers.

Preliminary measurements of the mean flow in a similar tee with a round edge between the main and branch pipes were also presented and showed a shorter, thinner and weaker recirculation bubble, suggesting that lower local loss coefficients will be determined in the pressure measurements that are about to be carried out.

ACKNOWLEDGEMENTS

The authors would like to acknowledge the financial support of JNICT through project PBIC/C/CEG/2440/95. A. Schulte would also like to thank the Leonardo da Vinci programme of the European Union for the scholarship that allowed his stay at INEGI. The authors are listed alphabetically.

REFERENCES

Boldy, A. P. 1970, Performance of Dividing and Combining Tees. BHRA Technical report 1061.

Gardel, A. 1957, Les Pertes de Charge dans les Écoulements au Travers de Branchements en Té. Bulletin Technique de la Suisse Romande, n° 9 and 10.

Gyr, A. and Bewersdorff, H.- W. 1995, Drag Reduction of Turbulent Flows by Additives. Kluwer Academic Publishers, Dordrecht.

Idel'cik, 1986, Handbook of Hydraulic Resistance, Hemisphere Publishing Company, New York.

Ito, H. and Imai, K. 1973, Energy Losses at 90° Pipe Junctions, Journal of the Hydraulics Division, Proceedings of the ASCE, Vol. 99, n° HY9.

Maia, R. 1992, Investigações Numéricas e Experimentais do Efeito das Perdas de Carga Localizadas em Sistemas de Tubagens. Métodos e Técnicas para o Seu Estudo Sistemático. O Caso Particular do Tê a 90°, PhD Thesis, University of Porto.

Miller, D. S. 1986, Internal Flow Systems, BHRA Fluid Engineering, 3rd edition.

Sierra-Espinosa, F. Z. and Bates, C. J. 1997, Prediction and Measurement of a Turbulent Flow in a 90° Pipe Junction, Proc. of the V Encontro Nacional de Mecânica Computacional, Guimarães, Portugal, vol. 2, pp 945-955.

Stieglmeier, M. and Tropea, C. 1992, A Miniaturized, Mobile Laser-Doppler Anemometer, Applied Optics, vol. 31, pp 4096.

VDI (Verin Deutcher Ing.) 1984. Druckverlust, VDI- Warmeatlas, VDI Verlag, Dusseldorf.